

#### Contents lists available at ScienceDirect

# Energy

journal homepage: www.elsevier.com/locate/energy



# A highly efficient combined multi-effect evaporation-absorption heat pump and vapor-compression refrigeration part 2: Thermoeconomic and flexibility analysis



Iman Janghorban Esfahani, Changkyoo Yoo\*

Dept. of Environmental Science and Engineering, College of Engineering, Center for Environmental Studies, Kyung Hee University, Seocheon-dong 1, Giheung-gu, Yongin-Si, Gyeonggi-Do, 446-701, Republic of Korea

#### ARTICLE INFO

Article history: Received 17 February 2014 Received in revised form 16 July 2014 Accepted 24 July 2014 Available online 19 August 2014

Keywords: Absorption Combined system Desalination Refrigeration Thermoeconomic

#### ABSTRACT

This paper continues Part 1 of our study and develops a thermoeconomic model of the system with low and high pressure compressors. The thermoeconomic model was used to assess the unit cost of the fresh water and cooling and to evaluate the flexibility of the system for fuel allocation from different electricity and heat energy sources. A parametric analysis was carried out to investigate the effects of the RR (refrigerant flow-rate ratio) from the high pressure compressor to the low pressure compressor of the VCR (vapor compression refrigeration) system, the price of steam, and the price of electricity on the product cost rate and the exergy efficiency of the system. The results showed that the system with two compressors had high flexibility to allocate the different energy sources when the availability of the sources was limited for a given value of fresh water and cooling production.

© 2014 Elsevier Ltd. All rights reserved.

## 1. Introduction

Fresh water and refrigeration are two important products that are usually required simultaneously in many regions with hot and dry climates such as Middle Eastern countries. In order to decrease the product cost rate of fresh water and refrigeration production and to increase the performance of the fresh water and refrigeration production processes, a new configuration of a combined system has been introduced in Part 1 of this paper. This system combines the MEE-ABHP (multiple effects evaporation-absorption heath pump) desalination system with the VCR (vapor compression refrigeration) cycle. In Part 1 of this two-part paper, the energy and cost performances of the proposed combined systems with the refrigeration ratio values of 0, 0.5, and 1 were investigated and compared to the stand-alone MEE-ABHP, and VCR systems by developing model-based energy and cost. In Part 2 of this paper, since the combined system produces two products including fresh water and refrigeration the thermoeconomic model was developed in order to calculate the product cost rates to investigate the thermoeconomic performance and the flexibility of the system, which cannot be achieved by model-based energy and economics.

DOI of original article: http://dx.doi.org/10.1016/j.energy.2014.07.081.

Thermoeconomics combines the principle of thermodynamics and economics in order to provide useful information on cost effective energy conversion systems that is not usually available through conventional energy and economic modeling [1]. The thermoeconomic approach is used to distribute the cost of the entire process onto the internal process streams based on exergy not energy. The monetary cost of the process streams, specifically the cost of product streams, in thermoeconomic analysis were calculated by the stream-cost equations that are arranged in a matrix form [2,3].

Recently, several researchers have studied thermoeconomic modeling of seawater desalination, refrigeration, and combined systems [1–11]. Farshi et al. [1] performed exergoeconomic analysis for the series flow double effect and combined ejector double effect systems in order to investigate and compare the influences of various operating parameters on the investment costs of the overall systems and the product cost flow rates. Hosseini et al. [2] considered the effects of equipment reliability in their thermoeconomic analysis of a combined power and multi stage flash water desalination plant. They developed an economic model according to the total revenue requirement method. Zare et al. [4] investigated and optimized the performance of an ammonia-water/cooling cogeneration cycle and they focused on the economic point of view. Their results showed that the sum of the unit costs of the cycle products obtained through thermoeconomic optimization

<sup>\*</sup> Corresponding author. Tel.: +82 31 201 3824; fax: +82 31 202 8854. E-mail address: ckyoo@khu.ac.kr (C. Yoo).

was approximately 18.6% and 25.9% less than that in the cases when the cycle was optimized from the viewpoints of the first and second laws of thermodynamics, respectively. Wang and Lior [5] analyzed the thermal and economic performance of a LT-MEE (low temperature-MEE) water desalination system coupled with a LiBr-H $_2$ O absorption heat pump. Their results showed that a 67–78% increase in water production over a stand-alone LT-MEE run in the same heat source conditions can be obtained due to the coupling. As noted in the literature, thermoeconomic analysis should be carried out to analyze the proposed system for better understanding of the system, because exergy reflects the measures of the processes.

This part of our two-part paper contributes to the thermoeconomic analysis of the combined MEE-ABHP-VCR system with low and high pressure compressors in order to investigate the thermo-economic performance and flexibility of the proposed system in fuel allocation from different energy sources. Part 2 of this paper consists of four major parts. First, the thermodynamic properties of the system were specified using the thermodynamic model developed in the first part of this paper. Second, exergy analysis was conducted in order to determine the exergy destruction, exergy loss, exergetic efficiency, and exergy destruction ratio as the energy performance criterion. Third, thermoeconomic analysis was conducted in order to calculate the thermoeconomic variables and to present the suggested design guidelines for potential cost-effective improvements for the system. Forth, the effects of the refrigerant flow-rate ratio from the low pressure compressor to the high pressure compressor (RR) and the price of the energy sources, including electric power and heat energy, on the product cost rates of the system were investigated in order to investigate the flexibility of the system for the allocation of the different energy sources.

## 2. Materials and methods

## 2.1. System configuration

The system presented in Fig. 1 was suggested as a replacement of a portion of the required energy for the MEE system with electric

power. In the proposed system, the condenser of the VCR system was replaced with the MEE-ABHP desalination system in order to recover the waste heat from the VCR condenser as a heat energy source for the MEE system. For this purpose, a portion of the fresh water produced in the last stage of the MEE-ABHP system (which has lower pressure than the other stages) was used as a refrigerant for the VCR system. The refrigerant was expanded through the expansion valve (EV<sub>2</sub>) and passed through the evaporator. The refrigerant coming from the evaporator was divided into two parts: one part was compressed by the low pressure compressor and sent to the absorber, and the other part was compressed by the high pressure compressor and sent to the tube side of the first stage of the MEE subsystem as an energy source. The high pressure compressor operated as a mechanical heat pump for the MEE subsystem, which could reduce the heat energy consumption of the MEE system and consume electric power instead of the motive steam flow rate in order to produce fresh water. Therefore, the combined system with two compressors had the flexibility to allocate heat energy and electric power energy as energy sources. The initial circumstances for operating and the thermodynamic parameters for the MEE-ABHP-VCR system presented in Fig. 1 are presented in Table 1.

#### 2.2. Exergy analysis of the system

Exergy analysis is essential to identify the location, source, and magnitude of the true thermodynamic inefficiencies and to assess the thermoeconomic behavior of the energy converting systems [1,2]. Exergy can be divided into kinetic, potential, physical, and chemical exergies. Chemical exergy is an important part of exergy in combustion processes. Neglecting the kinetic and potential exergies, the physical exergy is defined as the theoretical maximum of the useful work obtained as a system interacts in the equilibrium state that is given by the following Eq. (1) [12]:

$$\dot{E}x_{\rm ph} = \dot{m} \cdot ((h - h_0) - T_0(s - s_0)),\tag{1}$$

where m is the mass flow rate, h is the specific enthalpy, s is the specific entropy, T is the absolute temperature (K), and (0) refers to

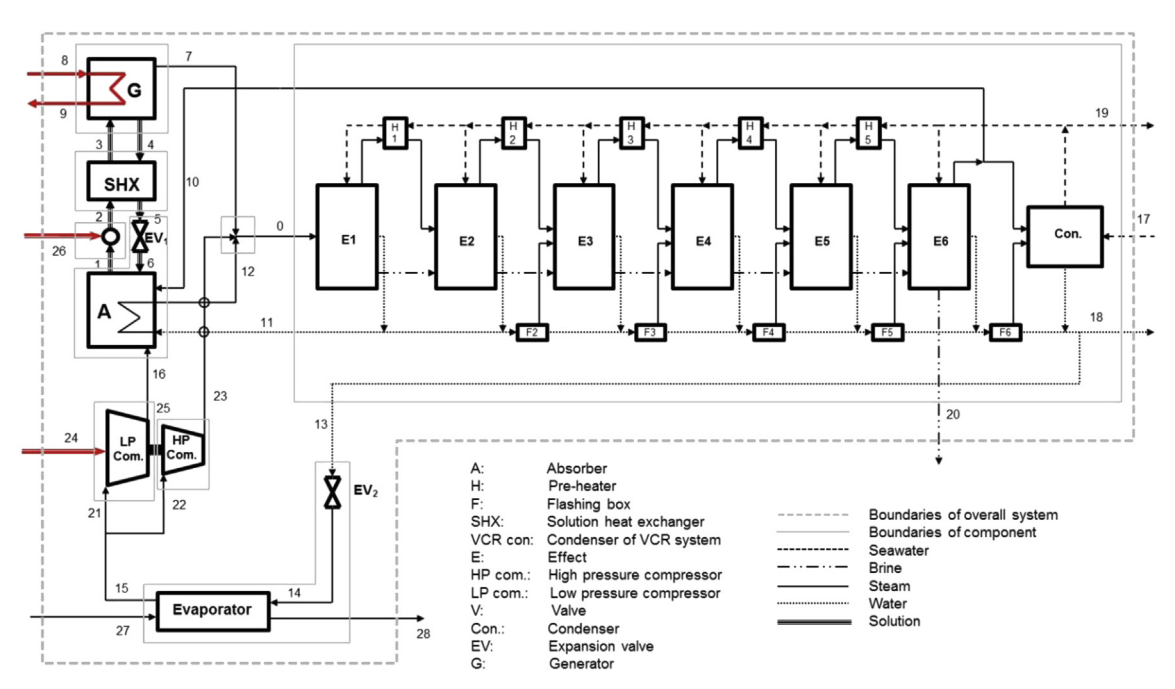


Fig. 1. Schematic of the proposed combined MEE-ABHP system with a VCR system with two compressors.

**Table 1**Initial circumstances for operating and thermodynamic parameters for the MEE-ABHP-VCR system.

Parameter	Value	Units
$P_A$	7.5	kPa
Effect number	6	_
$\Delta T_{ m MEE}$	3	°C
P <sub>motive</sub> steam	500	kPa
$\eta_{ m com}$	91	%
$X_{sw}$	30,000	ppm
$X_{\mathrm{B6}}$	70,000	ppm
$T_1$	79.2	°C
$T_4$	117.4	°C
$T_{14}$	6	°C
Qfresh water	15,000	m <sup>3</sup> /d
Q <sub>cooling</sub>	30,000	kW
Steam price	11	\$/ton
Electric price	0.07	\$/kWh

the ambient conditions. The reference temperature for the all cases is considered as 25  $^{\circ}\text{C}.$ 

The specific entropy and enthalpy of the seawater at a specified temperature T and pressure P are determined as follows:

$$h_{\text{seawater}} = mf_s h_s + mf_w h_w \tag{2}$$

and

$$s_{\text{seawater}} = mf_s s_s + mf_w s_w, \tag{3}$$

where the subscripts s and w represent salt and water, and mf is the mass fraction. The assumed conditions of the environment are as follows. The environmental temperature of 25 °C, one atmospheric pressure, and a salinity of 0.042% for seawater are considered to be the ambient environmental state for the system. The specific heat, the enthalpy, and the entropy of the salt at the ambient state can be determined by the following Eqs. (4) and (5) [13]:

$$h_s = h_{s0} + cp_s(T - T_0) = 20.92 + 0.8368(T - 298)$$
 (4)

and

$$s_s = s_{s0} + cp_s \ln(T/T_0) = 0.0732978 + 0.8368 \ln(T/298).$$
 (5)

The enthalpy and entropy for water-LiBr have been evaluated by the correlations from Ref. [14] which are presented in Appendix-A.

The exergy destruction, exergetic efficiency, exergy destruction ratio, and exergy loss ratio in each component of the system as the detailed exergy analysis are given by Eqs. (6)–(9) [15]:

$$\dot{E}_{D,k} = \dot{E}_{F,k} - \dot{E}_{P,k} - \dot{E}_{L,k},\tag{6}$$

$$\varepsilon_{k} = \frac{\dot{E}_{p,k}}{\dot{E}_{F,k}} = 1 - \left[ \frac{\left( \dot{E}_{D,k} + \dot{E}_{L,k} \right)}{\dot{E}_{F,k}} \right],\tag{7}$$

$$Y_{D,k} = \frac{\dot{E}_{D,k}}{\dot{E}_{E \text{ total}}}, \tag{8}$$

and

$$Y_{L,k} = \frac{\dot{E}_{L,k}}{\dot{E}_{F,\text{total}}},\tag{9}$$

where *E* represents the exergy rate. *D*, *F*, *P*, *L* and *k* refer to the destruction, fuel, product, loss and component, respectively. In order to define the fuel, product, and loss exergy of each

component and overall system the boundaries of each component and overall system are shown in Fig. 1.

#### 2.3. Thermoeconomic analysis of the system

Thermoeconomic analysis was used to reveal the cost formation processes and to calculate the cost exergy unit of the product streams of the system [4]. In order to calculate the cost rate of each stream in the system, the cost balance was applied to each component of the cycle as given by the following Eq. (10):

$$\sum \dot{C}_{\text{in},k} + \dot{Z}_{k}^{CI} + \dot{Z}_{k}^{OM} = \sum \dot{C}_{\text{out},k},$$
(10)

where  $C_{\rm in}$ , and  $C_{\rm out}$  are the cost rates associated with the streams to/from the component and  $Z^{CI}$  and  $Z^{OM}$  are the related cost of capital investment and operating and maintenance for the kth component obtained using the economic model presented in Part 1 of this paper [2]. In the application of the cost balance equation (Eq. (10)) there is usually more than one inlet-outlet stream for some of the components. Therefore, the number of unknown cost parameters is higher than the number of cost balance equations for the component. In order to solve this problem, auxiliary thermodynamic equations were developed according to the P and F rules [2]. Based on these rules, the product was defined as being equal to the sum of all of the exergy values that were taken into consideration at the outlet plus all of the increases in the exergy between the inlet and outlet that were in accordance with the purpose of the component. Similarly, the fuel was defined as being equal to all of the exergy values that were taken into consideration at the inlet plus all of the decreases in the exergy between the inlet and outlet minus all of the exergy increases that were not in accordance with the purpose of the component [16]. Since the throttling valves were the components for which a product could not be readily defined, the EV1 and the absorber, which was served by the EV1, were considered to be a single component, and the EV2 and the evaporator, which was served by the EV2, were considered to be a single component [15,17]. These considerations led to the fuel, product, and loss definitions for the system component that are summarized in Table 2.

The formulation of the cost balances and the required auxiliary equations for each component are given by Eqs. (11)–(30) as follows:

Generator:

$$\dot{C}_4 + \dot{C}_7 + \dot{C}_9 = \dot{C}_8 + \dot{C}_3 + \dot{Z}_G, \tag{11}$$

$$\frac{\dot{C}_4 - \dot{C}_3}{\dot{E}_4 - \dot{E}_3} = \frac{\dot{C}_7 - \dot{C}_3}{\dot{E}_7 - \dot{E}_3},\tag{12}$$

SHX

$$\dot{C}_3 + \dot{C}_5 = \dot{C}_2 + \dot{C}_4 + \dot{Z}_{SHX},\tag{13}$$

**Table 2** Fuel-Product-Loss definition of the MEE-ABHP-VCR system.

Component	Fuel	Product	Loss
Generator	$\dot{E}_8 - \dot{E}_9$	$\dot{E}_7 + \dot{E}_4 - \dot{E}_1$	_
SHX	$\dot{E}_4 - \dot{E}_5$	$\dot{E}_3 - \dot{E}_2$	_
Pump	$\dot{W}_{ m pump}$	$\dot{E}_2 - \dot{E}_1$	_
Absorber-EV1	$\dot{E}_5 + \dot{E}_{10} + \dot{E}_{16} - \dot{E}_1$	$\dot{E}_{12} - \dot{E}_{11}$	_
LP,com.	$\dot{W}_{ ext{LP}}$	$\dot{E}_{16} - \dot{E}_{21}$	_
HP,com.	$W_{\mathrm{HP}}$	$\dot{E}_{23} - \dot{E}_{22}$	_
Evaporator-EV2	$\dot{E}_{13} - \dot{E}_{15}$	$\dot{E}_{28} - \dot{E}_{27}$	_
MEE	$\dot{E}_0 - \dot{E}_{11} - \dot{E}_{13} - \dot{E}_{10}$	Ė <sub>18</sub>	$\dot{E}_{19} + \dot{E}_{20}$
Overall	$\dot{E}_8 - \dot{E}_9 + \dot{W}_{\text{pump}} + \dot{W}_{\text{LP}} + \dot{W}_{\text{HP}}$	$\dot{E}_{18} + \dot{E}_{28} - \dot{E}_{27}$	$\dot{E}_{19} + \dot{E}_{20}$

$$c_4 = c_5,$$
 
$$c_{F,k} = \frac{\dot{C}_{F,k}}{E_{F,k}},$$

$$\dot{C}_1 + \dot{C}_{26} + \dot{Z}_{pump} = \dot{C}_2,$$
Evaporator-EV1:
$$c_{p,k} = \frac{\dot{C}_{p,k}}{E_{p,k}},$$
(32)

$$\dot{C}_{15} + \dot{C}_{28} = \dot{C}_{13} + \dot{C}_{27} + \dot{Z}_{Eva} + \dot{Z}_{EV1}, \tag{16} \qquad \dot{C}_{D,k} = c_{F,k} \dot{E}_{D,k}, \tag{33}$$

$$c_{14} = c_{15},$$
 (17)  $\dot{C}_{I,k} = c_{F,k} \dot{E}_{I,k},$  (34)

$$r_{k} = \frac{c_{p,k} - c_{F,k}}{c_{F,k}} = \frac{C_{D,k} + Z_{k}}{c_{F,k}E_{p,k}} = \frac{1 - \varepsilon_{k}}{\varepsilon_{F,k}E_{p,k}} + \frac{Z_{k}}{\varepsilon_{F,k}E_{p,k}},$$
(35)

$$c_{27} = 0, (19)$$

Absorber-EV2:

$$\dot{C}_{11} + \dot{C}_{10} + \dot{C}_5 + \dot{C}_{16} + \dot{Z}_{Abs} + \dot{Z}_{EV2} = \dot{C}_1 + \dot{C}_{12}, \qquad (20) \qquad f_k = \frac{\dot{Z}_k}{\dot{Z}_k + \left(\dot{C}_{D,k} + \dot{C}_{L,k}\right)}.$$

$$\frac{\dot{C}_6 + \dot{C}_{10} + \dot{C}_{16}}{\dot{E}_6 + \dot{E}_{10} + \dot{E}_{16}} = \frac{\dot{C}_1}{\dot{E}_1} , \tag{21}$$

$$c_5 = c_6, \tag{22}$$

Low pressure compressor:

$$\dot{C}_{21} + \dot{C}_{24} + \dot{Z}_{com.LP} = \dot{C}_{16},\tag{23}$$

High pressure compressor:

$$\dot{C}_{22} + \dot{C}_{25} + \dot{Z}_{com.HP} = \dot{C}_{23},$$
 (24)

Mivor

$$\dot{C}_7 + \dot{C}_{23} + \dot{C}_{12} = \dot{C}_0, \tag{25}$$

Splitter:

$$\dot{C}_{15} = \dot{C}_{21} + \dot{C}_{22},\tag{26}$$

$$c_{21} = c_{22}, (27)$$

MEE:

$$\dot{C}_0 + \dot{C}_{17} + \dot{Z}_{MEE} = \dot{C}_{19} + \dot{C}_{11} + \dot{C}_{10} + \dot{C}_{18} + \dot{C}_{20} + \dot{C}_{13}, \tag{28}$$

$$c_{17} = c_{20} = c_{19} = 0, (29)$$

and

$$c_{11} = c_{13} = c_{10} = c_0. (30)$$

The linear system in Eqs. (11)–(30) includes 28 variables  $[X] = \{\dot{C}_1, \dot{C}_2, ..., \dot{C}_{27}, \dot{C}_{28}\}$  that can be solved in order to obtain the unit exergetic cost of all of the exergy streams of the system by taking into consideration the cost of the steam used in the generator and the electrical energy used for the pump and compressors as 11 \$/ton, and 0.07 \$/kWh, respectively. The thermoeconomic variables, which play a very important role in evaluating the thermoeconomic performance and improvement potentials of thermal systems, are the average unit cost of fuel,  $c_f$ , the average unit cost of product,  $c_p$ ; the cost rate of exergy destruction,  $C_D$ ; the cost rate of exergy loss, C<sub>l</sub>; the relative cost difference, r; and the exergoeconomic factor, f; which are given by the following Eqs. (31)–(36) [15]:

## 3. Results and discussion

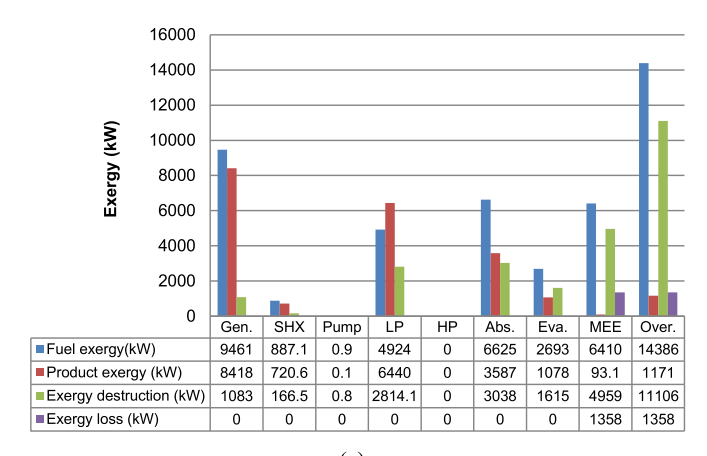
3.1. Exergy analysis

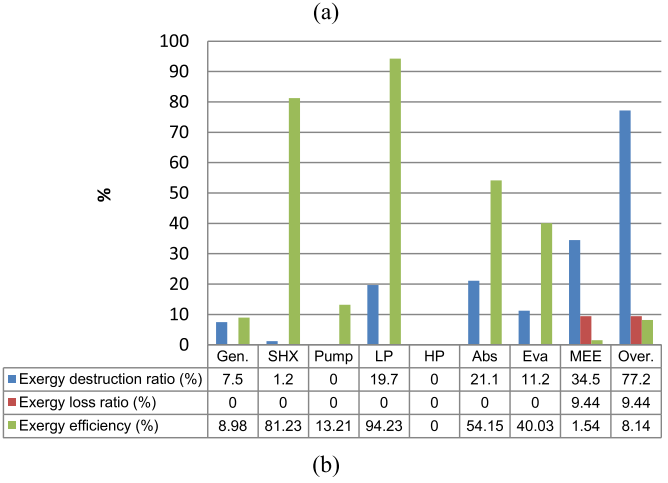
The thermodynamic model presented in Part 1 of this paper was used to calculate the thermodynamic properties of three MEE-ABHP-VCR systems with refrigerant flow-rate ratio from low pressure compressor to high pressure compressor (RR) values of 0, 0.5, and 1, which indicate that the system operates with a low pressure compressor, low and high pressure compressors, and a high pressure compressor, respectively. The exergy analysis of the three combined systems and their components was performed using the presented F-P-L relationships and Eqs. (1)–(9) in order to calculate the exergy destructions and the detailed exergy analysis of the components.

(31)

The simulation results MEE-ABHP-VCR system with RR values of 0, 0.5, and 1 are presented in Tables B-1-B-3 in Appendix-B and the exergy analysis results are presented in Figs. 2-4. As shown in Fig. 2 for the system with RR = 0, the maximum exergy destruction of 4959 kW occurred in the MEE subsystem, which was 34.47% of the total fuel exergy of the system. The absorber had the second largest exergy destruction of 3038 kW with an exergy destruction ratio of 21.12%, which indicates that 21.12% of the total fuel exergy was destructed by the absorber. These two subsystems were followed by the low pressure compressor, evaporator, generator, solution heat exchanger, and pump with exergy destructions of 2814.1, 1,615, 1,083, 166.5, 0.809 kW, respectively, and exergy destruction ratios of 19.56%, 11.23%, 7.53%, 1.157%, and 0.0056%, respectively. Also, among all of the components, MEE just lost the exergy of 1358 kW by discharging the brine and cooling water to the environment. It could be seen that the fuel exergy of the generator and the low pressure compressor as two of the energy sources of the system were 9461 kW, and 4924 kW. Therefore, we concluded that since the fuel exergy of the generator was higher than that of the compressor, then the heat energy consumption of the system was higher than the electric energy. As shown in Fig. 2b the overall exergy efficiency of the system was 8.14% when the low pressure compressor had the highest exergy efficiency of 94.23% and the MEE had the lowest exergy efficiency of 1.54% among all of the system components.

Fig. 3 shows the exergy analysis results of the MEE-ABHP-VCR system with RR = 0.5, the MEE subsystem destructed the maximum value of the exergy among all of the components at

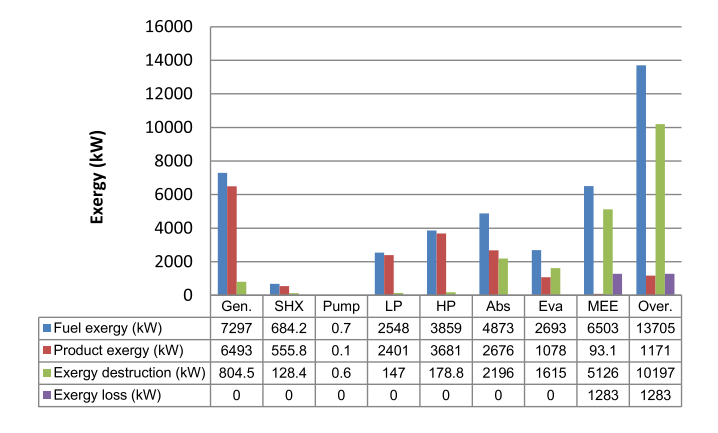




**Fig. 2.** Exergy analysis results of the MEE-ABHP-VCR system with RR = 0; a) Fuel exergy, product exergy, exergy destruction, and exergy loss; b) Exergy destruction ratio, exergy loss ratio, and exergy efficiency.

5126 kW, which was 37.4% of the total fuel exergy of the system. It also lost 1283 kW exergy by discharging of the exergy to the environment through discharging brine and cooling water to the sea. The absorber, evaporator, generator, high pressure compressor, low pressure compressor, solution heat exchanger, and pump had the highest to lowest exergy destruction with destruction of 16.02, 11.76, 5.87, 1.304, 1.073, 0.937, and 0.0045% of the total fuel exergy, which were 2,196, 1,615, 804.5, 178.8, 147, 128.4, and 0.6238 kW exergy, respectively. As shown in Fig. 3b, the overall exergy efficiency of the system was 8.544%. Among all of the components of the system, the high pressure compressor and the MEE had the highest and lowest exergy efficiencies of 95.37% and 1.43%, respectively.

Fig. 4 shows the exergy analysis results of the MEE-ABHP-VCR system with RR = 1. Since the RR was equal to 1, the system operated with just the high pressure compressor. As shown in Fig. 4a and b the MEE subsystem had the highest exergy destruction of 5683 kW with an exergy destruction ratio of 43.8% and lost 1204 kW of the exergy by discharging the exergy to the environment. The next component with the highest exergy destruction was the evaporator with exergy destruction of 1615 kW and an exergy destruction ratio of 12.45%. The absorber, generator, high pressure compressor, solution heat exchanger, and pump had the highest to lowest values of exergy destruction at 1,293, 548.7, 370.5, 87.57, and 0.4254 kW, respectively, and exergy destruction ratio values of 9.968%, 4.228%, 2.855%, 0.675%, and 0.0032%, respectively. As shown in Fig. 4b, the overall exergy efficiency of the system was



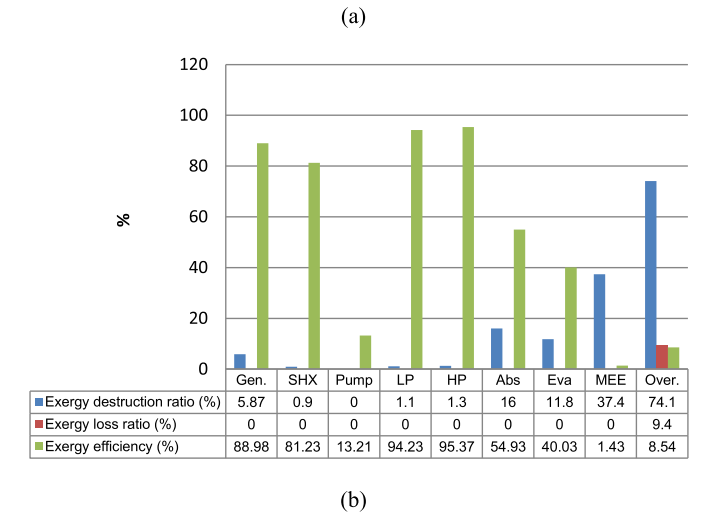
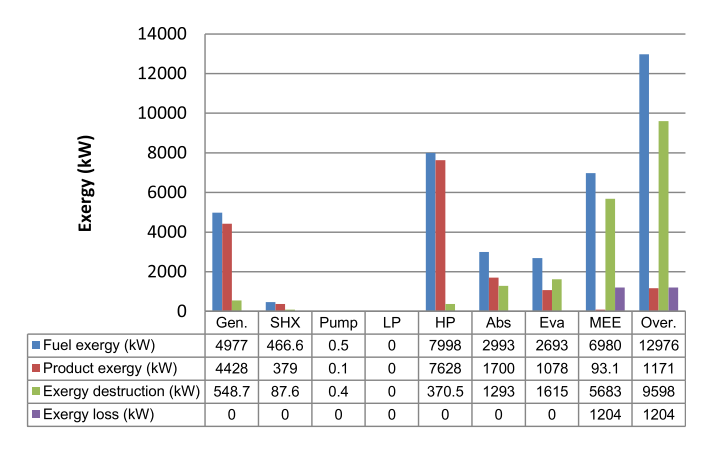


**Fig. 3.** Exergy analysis results of the MEE-ABHP-VCR system with RR = 0.5; a) Fuel exergy, product exergy, exergy destruction, and exergy loss; b) Exergy destruction ratio, exergy loss ratio, and exergy efficiency.

9.024%. The high pressure compressor and the MEE had the highest and lowest exergy efficiency among all of the components of the system at 95.37% and 1.33%, respectively.

In three of the combined systems, the reason for the exergy destructions of each component could be explained by irreversibilities and exergy losses. The exergy destructed in the MEE subsystem was due to two reasons. Of the first reason was the heat transfer temperature difference between the hot and cold streams, which resulted in the irreversibility of the process and the second was discharging the exergy by discharging the brine and the cooling water into the environment. The exergy destruction of the heat exchangers including the absorber, generator, solution heat exchanger, and evaporator was due to the irreversibility due to the heat transfer temperature difference between the hot and cold streams. The exergy destruction of the pump and high pressure compressor was due to the irreversibility of the compression process. However, the value of the exergy destruction of the pump was negligible.

By comparing the exergy analysis results of the three MEE-ABHP-VCR systems, it was found that the fuel of the generator and the low pressure compressor decreased with an increase in the RR, while the fuel of the high pressure compressor increased. The reason was that the share of the high pressure compressor in the compressing of the refrigerant coming from the evaporator increased with an increase in the RR value, which lead to an increase in the high pressure compressor share in order to prepare



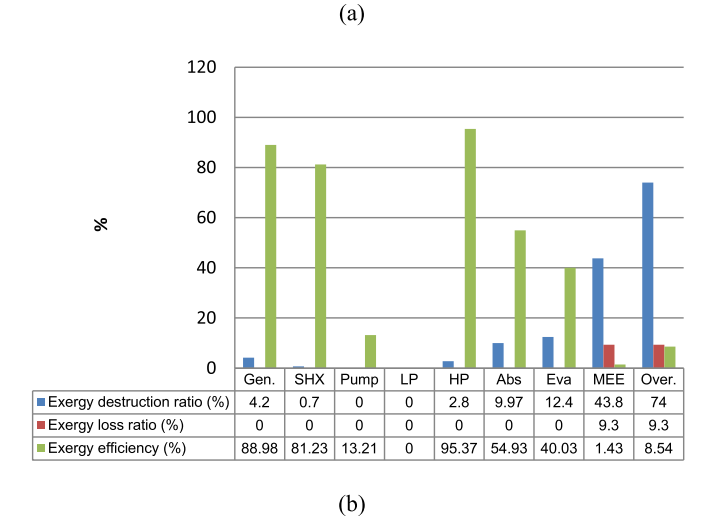


**Fig. 4.** Exergy analysis results of the MEE-ABHP-VCR system with RR = 1; a) Fuel exergy, product exergy, exergy destruction, and exergy loss; b) Exergy destruction ratio, exergy loss ratio, and exergy efficiency.

the requirement energy of the desalination system. From Figs. 2-4, it can be seen that the fuel exergy of the SHX, pump, absorber, and overall system decreased with an increase in the RR, while the fuel exergy of the MEE increased. This can be explained by the fact that since the SHX, absorber, and pump were the components of the ABHP subsystem, the load of these components were directly affected by the load of the generator. Therefore, the fuel exergy of those components decreased with an increase in the RR and a decrease in the fuel exergy of the generator. The reason for the increase in the fuel exergy of the MEE was that the exergy product of the high pressure compressor, which provided a portion of the fuel exergy of the MEE, increased with an increase in the RR. In addition, it was found that since the cooling load and operation conditions of the evaporator were considered constant, then the fuel and product exergy of the evaporator didn't change with an increase in the RR.

When comparing the exergy destruction of the components, it was found that the exergy destruction of the generator decreased with an increase in the RR. An increase in the RR caused the load of the generator to decrease, which resulted in a decrease in the exergy destruction and, consequently, a decrease in the exergy destruction of the SHX, absorber, and pump. The exergy destruction of the MEE increased with the increase in the RR, because the fuel exergy of the MEE increased while the product exergy didn't change and the exergy loss decreased with an increase in the RR.

As presented in Figs. 2—4, the exergy efficiency of the generator, SHX, pump, low pressure compressor, high pressure compressor, and evaporator was constant with an increase in the RR, while the exergy efficiency of the absorber increased and the exergy efficiency of the MEE decreased with an increase in the RR value. Also the overall exergy efficiency of the system increased with an increase in the RR.

## 3.2. Exergoeconomic analysis

The exergoeconomic analysis was performed using the method described by Bejan et al. [18] in order to assess the performance of the combined system thermo-economically. The analysis was carried out using Eqs. (11)—(36) in order to define the average unit cost of the fuel,  $c_f$ ; the average unit cost of products,  $c_p$ ; the cost rate of exergy destruction,  $C_D$ ; the relative cost difference, r; and the exergoeconomic factor, f; for each component of the system. The thermoeconomic results of the three MEE-ABHP-VCR systems with refrigerant flow-rate ratio values of 0, 0.5, and 1 are presented in Tables C-1—C-3 in Appendix-C and Figs. 5—7.

In designing a new system, the first design changes must initially be applied to the components for which the sum of  $C_D + C_L + Z$  is the highest [18]. Fig. 5 shows the value of  $C_D + C_L + Z$ of the three MEE-ABHP-VCR systems with RR = 0, 0.5, and 1. As shown in Fig. 5, the MEE and pump of three systems had the maximum and minimum values of  $C_D + C_L + Z$  among of all the components, respectively. The second component with the highest value of  $C_D + C_L + Z$  was the low pressure compressor of the system with RR = 0, and the high pressure compressor of the systems with RR = 0.5 and 1. The evaporator and the absorber were the third and the forth components with the highest value of  $C_D + C_L + Z$  of the three systems, respectively. The generator, and SHX had the next highest value of  $C_D + C_L + Z$  of the systems with RR = 0, and 1, respectively, whereas the low pressure compressor, generator, and SHX had the next highest value of  $C_D + C_L + Z$  of the system with RR = 0.5, respectively.

Figs. 6 and 7 show the values of exergoeconomic factor (f) and relative cost difference (r) of the three MEE-ABHP-VCR systems with RR = 0, 0.5, and 1. As presented in Figs. 6 and 7, the subsystems of MEE, evaporator, absorber, SHX, and the generator have a high value of r and a low value of f, where the system performance of the combined system can be improved. It is known that the performance of the combined energy system can be improved by decreasing the temperature difference between the effects of the MEE, decreasing the temperature difference between the hot and cold streams of the evaporator and the absorber, increasing the effectiveness of the SHX, and decreasing the

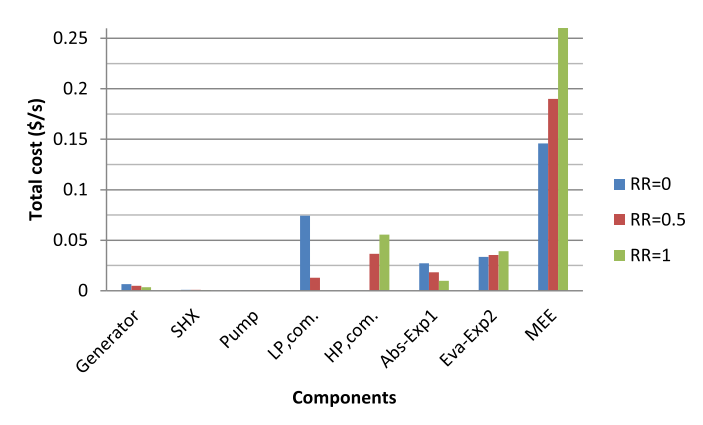
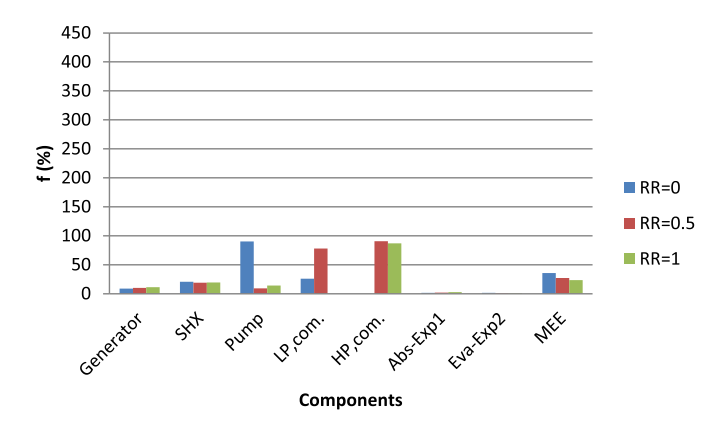


Fig. 5. Total cost values of the MEE-ABHP-VCR system with RR = 0, 0.5, and 1.



**Fig. 6.** Exergoeconomic factor (f) values of the MEE-ABHP-VCR system with RR = 0, 0.5, and 1.

temperature in the generator. Fig. 6 shows that the high pressure compressor and the pump had a low value of r and a high value of f. Therefore, it is straighforward to decrease the investment cost of the high pressure compressor at the expense of the exergy efficiency. As shown in Figs. 6 and 7, the r value of the low pressure compressor of the system with RR = 0 is higher than the f value, whereas its r value of the system with RR = 0.5 is lower than the f value. Therefore, the exergetic efficiency of the compressor of the system with RR = 0 should be increased with an increase in the capital investment cost and the investment cost of the low pressure compressor of the system with RR = 1 should be decreased at the expense of its exergy efficiency.

The effects of the refrigerant flow-rate ratio as the most significant parameter affecting the thermoeconomic performance of the system of the presented combined system could be determined by comparing the results presented in Figs. 5–7. As shown in Fig. 5 the  $C_D + C_L + Z$  value of MEE, evaporator, and high pressure compressor increased and the  $C_D + C_L + Z$  value of absorber, low pressure compressor, and generator decreased with an increase in RR. The effect of RR on the  $C_D + C_L + Z$  value of SHX, and pump was negligible. Since  $C_D + C_L + Z$  is the summation of the exergy destruction cost, exergy loss cost, and investment cost, then the decrease and increase in the value of  $C_D + C_L + Z$  of the components with an increase of RR can be explained by investigating the variations of the exergy destruction, investment cost, and exergy loss of the components with an increase in the RR.

The variations of the exergy destruction and exergy loss of the components is noted in Section 3.1 where the exergy analysis of the

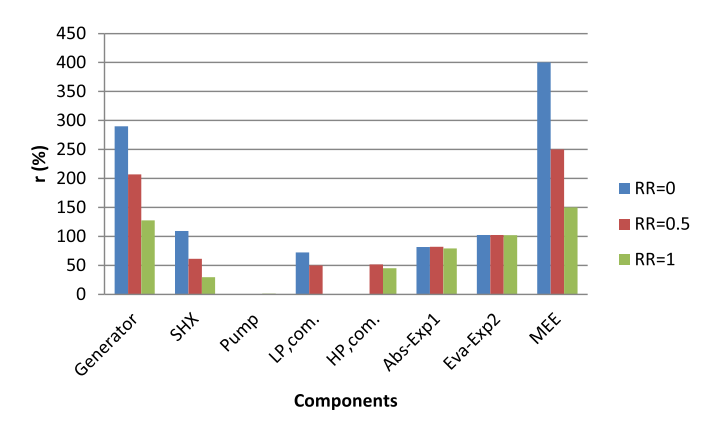


**Fig. 7.** Relative cost difference (r) values of the MEE-ABHP-VCR system with RR = 0, 0.5, and 1.

system was discussed. Since an increase in the RR caused a decrease in the load of the low pressure compressor and, therefore, that load of the ABHP subsystem that consisted of the generator, SHX, pump, and absorber were decreased, then the size of the components of the ABHP subsystem decreased, which led to a decrease in the investment capital cost.

The reasons for the increase in the investment cost of the high pressure compressor, the evaporator and the MEE were due to the increase in the size of these components by the increase in the refrigerant flow rate.

When comparing the f and r values of the components in Figs. 6 and 7, the f and r values of the MEE, high pressure compressor, evaporator, and SHX were decreased with an increase of the RR, where the values of r were higher than the values of f. The f and r values of the generator, absorber, low pressure compressor, and pump were increased with an increase of the RR, which resulted in the different decrease between the f and r values. However, the values of r were still higher than the values of f. Therefore, for the improvement of the exergetic efficiency of these components, the increase in the investment cost should be minimized with the high value of RR.

As presented in Tables C-1—C-3, the average unit product costs of the evaporator were 37.43, 43.76, and 48.45 \$/GJ and the average unit product costs of the MEE were 1,829, 2,063, and 2345 \$/GJ, respectively, for the system with RR values of 0, 0.5, and 1, where the combined systems showed the potential cost-effective improvements.

#### 3.3. Fuel allocation flexibility of the system

Note that the value of RR in the combined system determines the utilization values of the steam and electric power consumption of the system, where the unit costs of the steam and power are the main factors in the total cost of the products. It indicates that the fuel energy allocation of the steam and the electric power need to be evaluated when studying the flexibility of the systems. In this section, the effects of the steam and electric power prices was investigated under varying prices of the steam and the electric power along with the value of RR in the combined system in order to assess the flexibility of fuel allocation. It is known that the price of the steams depend not only on the steam pressure of the single fuel source but also the steam generation technology, the location, energy source used (renewable or non renewable) and energy source price of the different fuel sources [5]. In this paper, the values for the cost of the steam of 10, 11, 12, and 13 \$/ton were used for the steam price at the pressure of 500 MPa saturated steam, and 0.01, 0.04, 0.07, and 0.1 \$/kWh were used for the electric power costs in the thermoeconomic analysis [5].

Fig 8a-d show the results of fuel allocation flexibility of the system. Fig. 8a shows the effects of the different values of the electric power price and refrigeration ratio on the total product cost rate of the system at the fixed steam price of 10 \$/ton. As shown in Fig. 8a, the total product cost rate of the system increased with an increase in the value of RR and, at the fixed value of RR, the total product cost rate increased with an increase in the electric power price. At the higher values of the electric power cost, the effects of the RR on the total product cost were higher than at the lower values of the electric power cost, because the electric energy consumption of the high pressure compressor increased with an increase in the RR, which led to an increase in the total product cost. In addition, it was determined that the minimum total product cost could be achieved when the RR was equal to 0, which indicated that the system operated with just the low pressure compressor. Fig. 8b shows that the total product cost

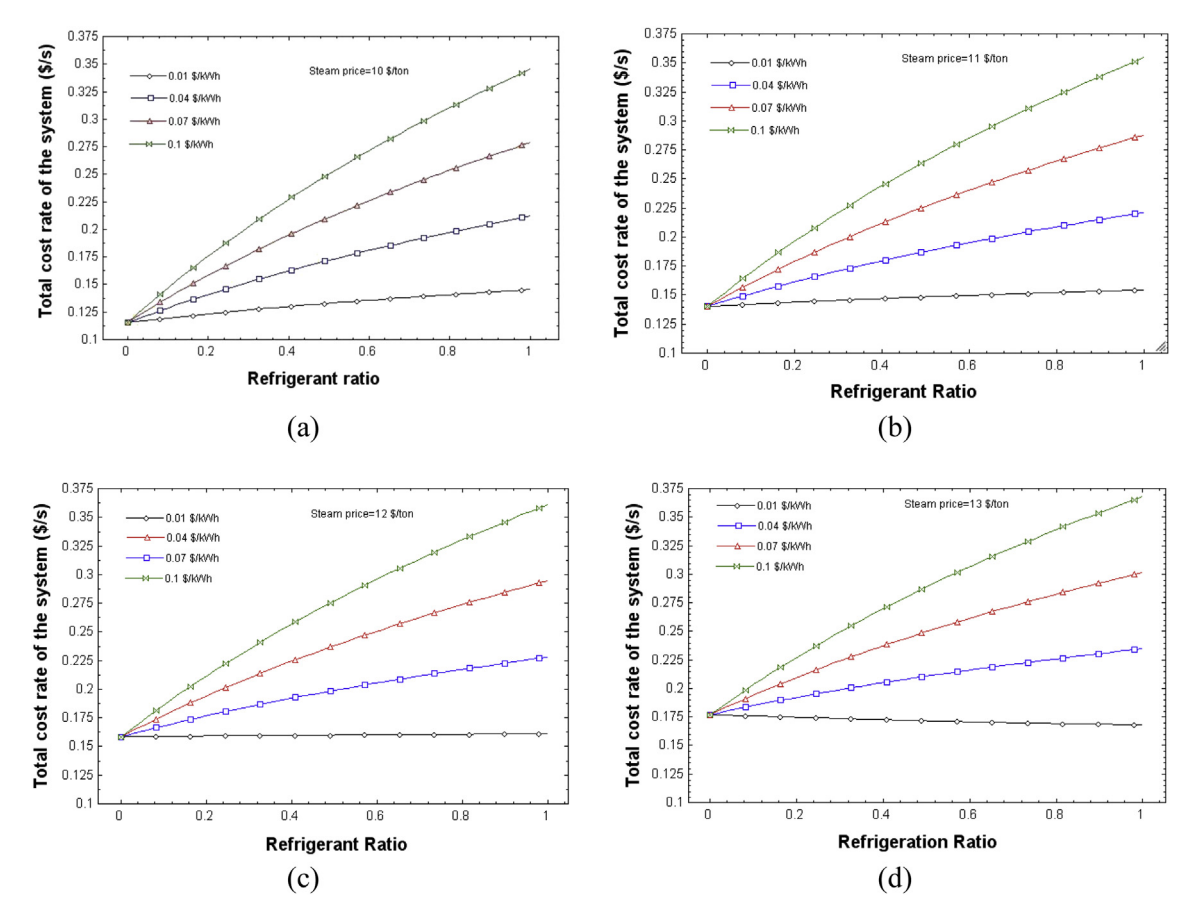


Fig. 8. Effects of the refrigerant flow-rate ratio, electric power price, and steam price on the total cost rate of the system with (a) steam price of 10 \$/ton, (b) steam price of 11 \$/ton, (c) steam price of 12 \$/ton, and (d) steam price of 13 \$/ton.

of the system increased with an increase in the RR and the electric power price at the fixed value of steam price of 11 \$/ton. In addition, the minimum value of the total product cost could be achieved when the system operated with just the low pressure compressor. However, the effects of the RR on the total product cost for the electric power price of 0.01 \$/kWh were very low. As shown in Fig. 8c, the total product cost of the system increased with an increase in the electric power price at the fixed value of steam price of 12 \$/ton. It was determined that, for the electric power prices of 0.1, 0.07, and 0.04 \$/kWh, the minimum total product cost of the system could be achieved when the system operated with the RR value equal to 0, which indicates that all of the refrigerant was compressed by the low pressure compressor. For the electric power price of 0.01 \$/kWh, the effects of RR were negligible, which indicates that the system had a high flexibility in the allocation of the heat energy and the electric power as energy sources without any changes in the total product cost of the system. Fig. 8d shows the effects of the different values of the electric power cost and the refrigeration ratio on the total product cost rate of the system at the fixed steam price of 13 \$/ton. It can be seen that, for electric power price of 0.1, 0.07, and 0.04 \$/kWh, the minimum total product cost of the system could be achieved when the system operated with the RR value equal to 0, while for electric price of 0.01 \$/kWh, the minimum total product cost of the system could be achieved when the system operated with a RR value equal to 1.

As shown in Fig 8, the average of the total product cost increased with an increase in the steam price. In addition, the interest in the system for allocating electric power as an energy source was higher than that of the steam source with an increase in the steam price

and a decrease in the electric power price. For an available steam of 13 \$/ton and an electric power of 0.01 \$/kWh, the purpose of the system was to consume electric power rather than steam, while the purpose of the system was to use steam instead of electric power for the electric power source of 0.04 \$/kWh. Therefore, we concluded that there are three primary reasons for using compressors for different values of steam price and electric power price. First, the electric power price was greater enough than the steam price, that the electric power consumption cost was higher than the steam consumption cost. Therefore, the low pressure compressor should be used in this case in order to compress all of the refrigerant coming from the evaporator to the absorber. Second, the steam price was greater enough than the electric power price, that the electric power consumption cost was lower than the steam consumption cost. In this case, the high pressure compressor was used to compressor all of the refrigerant coming from the evaporator to the tube side of the first effect of the MEE subsystem, which was a mechanical heat pump for the MEE subsystem that could reduce the heat energy consumption. Third, the electric power price and steam price were such that the electric power consumption cost and the steam consumption cost were equal to each other. In this case, both the low pressure and high pressure compressors could be used and the value of the RR could be defined based on the availability of the energy sources. In addition, both the low and high pressure compressors could be used in the first and second cases based on the availability of the energy sources. Therefore, the optimal value of the refrigerant flow-rate ratio should be defined in order to minimize the total product cost rate of the system based on the availability and prices of the energy sources.

#### 4. Conclusions

In Part 2 of this study, a MEE-ABHP-VCR system with two refrigerant compressors was proposed as a flexible system in order to allocate different energy sources. The exergy analysis was conducted in order to investigate the effects of the refrigerant flow-rate ratio from the low pressure compressor to the high pressure compressor on the exergy destruction and exergy efficiency of the system. The system was analyzed based on thermoeconomics in order to calculate the fresh water and the cooling cost rates as the products of the system and to investigate the fuel allocation flexibility of the system. The influences of the refrigerant flow-rate ratio and the energy source prices on the system product costs including steam and electric power were investigated. Compared to the systems with RR = 0.5, and 1, the overall cost rates of the combined MEE-ABHP-VCR system with RR = 0 was decreased and the exergy efficiency of the system was increased with an increase of the RR. In addition, the combined system with high and low pressure compressors showed the high flexibility which is able to allocate the different energy sources upon varying prices of the steam and the electric power.

#### Acknowledgments

This work was supported by the National Research Foundation of Korea(NRF) grant funded by the Korea government (NRF-2012R1A1B3001400)

## Appendix-A. Enthalpy and entropy of lithium bromide-water

The enthalpy of lithium bromide-water is calculated by Eq. (A.1) [14] which is valid for 0 < T < 190 °C and 40 < x < 75 wt.%

where x and T are solution concentration and temperature of lithium bromide-water, respectively.

### Appendix-B. Exergy analysis results

**Table B1** Results of the energy thermodynamic simulation for the MEE-ABHP-VCR system with RR=0.

State point	Pressure (kPa)	Temperature (C)	Mass flow rate (kg/s)	concentration	Specific enthalpy	Exergy kW
		_		(%)		
0	18.7	58.6	30.7	0	2641	6530.3
1	7.5	79.2	121.9	57.6	182.4	5808
2	18.7	79.2	121.9	57.6	182.4	5808.1
3	18.7	98.9	121.9	57.6	221.7	6528.7
4	18.7	117.4	108.8	64.6	282.5	11343.3
5	18.7	92.9	108.8	64. 6	238.5	10456.2
6	7.5	95	108.8	64. 6	238.5	10117.7
7	18.7	100.3	13.1	0	2686	2882.9
8	250	127.4	17.8	0	2717	10435.7
9	250	127.4	17.8	0	535.5	974.4
10	7.5	40.3	0.3	0	2574	23.1
11	18.7	58.6	17.6	0	245.5	90.8
12	18.7	58.6	17.6	0	2606	3678.1
13	7.5	40.3	12.8	0	168.8	6.9
14	0.9	6	12.8	0	168.8	-106.6
15	0.9	6	12.8	0	2512	-2685.9
16	7.5	208.7	12.8	0	2896	1953.7
17	101	30	2508	0	119.7	0
18	101	40.3	173.6	0	168.8	93.1
19	101	36.3	2161	0	144.9	526.6
20	101	55.6	173.6	0	154.4	830.9
21	0.9	6	12.8	0	2512	-2685.9
22	_	_	0	0	_	0
23	_	_	0	0	_	0
24	_	_	_	_	_	4923.7
25	_	_	_	_	_	0

$$\begin{aligned} h_{\text{LiBr-water}} &= \sum_{n=0}^{4} a_n x^n + T \sum_{n=0}^{3} b_n x^n + T^3 d_0 \\ a_0 &= -954.8, \quad a_1 = 47.7739, \quad a_2 = -1.59235, \quad a_3 = 2.09422 \times 10^{-2}, \quad a_4 = -7.689 \times 10^{-5} \\ b_0 &= -3.293 \times 10^{-1}, \quad b_1 = 4.076 \times 10^{-2}, \quad b_2 = -1.36 \times 10^{-5}, \quad b_3 = -7.1366 \times 10^{-6} \\ c_0 &= 7.4285 \times 10^{-3}, \quad b_1 = -1.5144 \times 10^{-4}, \quad b_2 = 1.3555 \times 10^{-6} \end{aligned} \tag{A.1}$$

where *x* and *T* are solution concentration and temperature of lithium bromide-water, respectively.

The entropy of lithium bromide-water is calculated by Eq. (A.2) [14] which is valid for  $0 \le T \le 190$  °C and.  $40 \le x \le 75$  wt.%

$$s_{\text{LiBr-water}} = a_1 + a_2 + a_3 T^2 + A_4 x + a_5 x T + a_6 x T^2 + a_7 x^2 + a_8 x^2 T + a_9 x^3 + a_{10} x^4$$

$$a_1 = -1.01961E3, \quad a_2 = 1.101529E - 1, \quad a_3 = -1.042150E - 2,$$

$$a_4 = 1.036935E2, \quad a_5 = -5.87032E - 2, \quad a_6 = 8.63107E - 5,$$

$$a_7 = -3.266802, \quad a_8 = -3.16683E - 4, \quad a_9 = 4.100993E - 2,$$

$$a_{10} = -1.790548E - 4$$
(A.2)

 $\label{eq:Table B2} \textbf{Results of the energy thermodynamic simulation of the MEE-ABHP-VCR system with RR = 0.5.}$ 

State point	Pressure (kPa)	Temperature (C)	Mass flow rate (kg/s)	LiBr concentration (%)	Specific enthalpy	Exergy kW
0	18.7	58.6	29.4	0	2745	6854
1	7.5	79.2	94	57.6	182.4	4479.7
2	18.7	79.2	94	57.6	182.4	4479.7
3	18.7	98.9	94	57.6	221.7	5035.6
4	18.7	117.4	83.9	64. 6	282.5	8749
5	18.7	92.9	83.9	64. 6	238.5	8064.8
6	7.5	95	83.9	64. 6	238.5	7803.7
7	18.7	100.3	10.1	0	2686	2223.5
8	250	127.4	13.7	0	2717	8049
9	250	127.4	13.7	0	535.5	751.5
10	7.5	40.3	3.5	0	2574	276.4
11	18.7	58.6	13.1	0	245.5	67.7
12	18.7	58.6	13.1	0	2606	2744.2
13	7.5	40.3	12.8	0	168.8	6.9
14	0.9	6	12.8	0	168.8	-106.6
15	0.9	6	12.8	0	2512	-2685.9
16	7.5	208.7	6.6	0	2896	1011
17	101	30	2204	0	119.7	0
18	101	40.3	173.6	0	168.8	93.1
19	101	36.3	1857	0	144.9	452.5 <del>4</del>
20	101	55.6	173.6	0	154.4	830.9
21	0.9	6	6.6	0	2512	-1389.9
22	0.9	6	6.2	0	2512	-1295.9
23	18.7	329.9	6.2	0	3136	2384.6
24	_	_	_	_	_	2548
25	_	_	_	_	_	3859.3

 $\label{eq:able B3} \textbf{Results of the energy thermodynamic simulation of the MEE-ABHP-VCR system with RR} = \textbf{1}.$ 

State point	Pressure (kPa)	Temperature (C)	Mass flow rate (kg/s)	LiBr concentration (%)	Specific enthalpy	Exergy kW
0	18.7	58.6	28		2868	7577.9
1	7.5	79.2	64.1	57.6	182.4	3055
2	18.7	79.2	64.1	57. 6	182.4	3055
3	18.7	98.9	64.1	57. 6	221.7	3434.1
4	18.7	117.4	57.2	64.6	282.5	5966.5
5	18.7	92.9	57.2	64. 6	238.5	5499.9
6	7.5	95	57.2	64. 6	238.5	5321.8
7	18.7	100.3	6.9	0	2686	1516.4
8	250	127.4	9.4	0	2717	5489.1
9	250	127.4	9.4	0	535.5	512.5
10	7.5	40.3	6.9	0	2574	548
11	18.7	58.6	8.3	0	245.5	43
12	18.7	58.6	8.3	0	2606	1742.6
13	7.5	40.3	12.8	0	168.8	6.9
14	0.9	6	12.8	0	168.8	-106.6
15	0.9	6	12.8	0	2512	-2685.9
16	_	_	_	_	_	_
17	101	30	1878	0	119.7	0
18	101	40.3	173.6	0	168.8	93.1
19	101	36.3	1531	0	144.9	373.1
20	101	55.6	173.6	0	154.4	830.9
21	_	_	_	_	_	_
22	0.9	6	12.8	0	2512	-2685.9
23	18.7	329.9	12.8	0	3136	4942.1
24	_	_	_	_	_	0
25	_	_	_	_	_	7998.5

## Appendix-C. Thermoeconomic analysis results

 $\label{eq:Table C1} \begin{tabular}{ll} \textbf{Table C1} \\ \textbf{Thermo-economic analysis results of the MEE-ABHP-VCR system with } RR = 0. \end{tabular}$ 

Component	$c_{F,k}$ (\$ GJ <sup>-1</sup> )	$c_{P,k}$ (\$ GJ <sup>-1</sup> )	$C_{D,k}$ (\$ s <sup>-1</sup> )	$C_{L,k}$ (\$ s <sup>-1</sup> )	$Z_k$ (\$ s <sup>-1</sup> )	$C_{D,k} + C_{L,k} + Z_k  (\$  s^{-1})$	f (%)	r (%)
Generator	5.5	21.5	0.0059	0	0.000566	0.00647	8.7	290
SHX	4	8.4	0.00067	0	0.000175	0.000844	20.7	109.4
Pump	19.4	19.5	0.000015	0	0.000001	0.0000165	9.1	0.26
LP,com.	19.4	33.5	0.055	0	0.01935	0.07435	26	72.3
HP,com.	0	0	0	0	0	0	0	0
Abs-Exp1	8.8	16	0.0267	0	0.00041	0.02711	1.5	81.5
Eva-Exp2	18.5	37.4	0.0298	0	0.000446	0.03346	1.3	102.4
MEE	18.5	1829	0.0916	0.0025	0.05174	0.14584	35.5	9791.8

Table C2 Thermo-economic analysis results of the MEE-ABHP-VCR system with RR = 0.5.

Component	$c_{F,k}$ (\$ GJ <sup>-1</sup> )	$c_{P,k}$ (\$ GJ <sup>-1</sup> )	$C_{D,k}$ (\$ s <sup>-1</sup> )	$C_{L,k}$ (\$ s <sup>-1</sup> )	$Z_k$ (\$ s <sup>-1</sup> )	$C_{D,k} + C_{L,k} + Z_k (\$ s^{-1})$	f(%)	r (%)
Generator	5.5	16.9	0.0044	0	0.0004843	0.00488	9.9	206.8
SHX	4.9	7.9	0.0063	0	0.000149	0.000779	19.1	61.3
Pump	19.4	19.5	0.00001	0	0.000001	0.000011	9.1	0.3
LP,com.	19.4	29.1	0.0028	0	0.01001	0.01281	78.14	49.9
HP,com.	19.4	29.5	0.0035	0	0.033	0.0365	90.4	51.6
Abs-Exp1	8.1	14.8	0.0178	0	0.000344	0.018144	1.9	81.9
Eva-Exp2	21.6	43.8	0.0349	0	0.000446	0.035346	1.3	102.2
MEE	21.6	2063	0.1109	0.0277	0.05132	0.189992	27	94.3

Table C3 Thermo-economic analysis results of the MEE-ABHP-VCR system with RR = 1.

Component	$c_{F,k}$ (\$ GJ <sup>-1</sup> )	$c_{P,k}$ (\$ GJ <sup>-1</sup> )	$C_{D,k}$ (\$ s <sup>-1</sup> )	$C_{L,k}$ (\$ s <sup>-1</sup> )	$Z_k$ (\$ s <sup>-1</sup> )	$C_{D,k} + C_{L,k} + Z_k  (\$  \mathrm{s}^{-1})$	f (%)	r (%)
Generator	5.5	12.5	0.00301	0	0.0003849	0.0033949	11.3	128
SHX	5.8	7.5	0.0005	0	0.0001189	0.0006189	19.2	29.4
Pump	19.4	19.6	0.000008	0	0.0000013	0.0000093	14	1
LP,com.	0	0	0	0	0	0	0	0
HP,com.	19.4	28.2	0.0072	0	0.04828	0.05548	87	45.1
Abs-Exp1	7.5	13.4	0.00965	0	0.00026	0.00991	2.6	79.3
Eva-Exp2	24	48.4	0.03872	0	0.000446	0.039166	1.1	102
MEE	24	234	0.13627	0.02887	0.05086	0.216	23.5	9678

#### References

- [1] Garousi Farshi L, Mahmoudi SMS, Rosen MA. Exergoeconomic comparison of double effect and combined ejector-double effect absorption refrigeration systems. Appl energy 2013;103:700-11.
- [2] Hosseini SR, Amidpour M, Behbahaninia A. Thermoeconomic analysis with reliability consideration of a combined power and multi stage flash desalination plant, Desalination 2011:278:424-33.
- Mabrouk AA, Nafey AS, Fath HES. Thermoeconomic analysis of some existing desalination processes. Desalination 2007;205:354–73.
- [4] Zare V, Mahmoudi SMS, Yari M, Amidpour M. Thermoeconomic analysis and optimization of an ammonia-water power/cooling cogeneration cycle. Energy 2012:47:271-83
- Wang Y, Lior N. Thermoeconomic analysis of a low-temperature bmulti-effect thermal desalination system coupled with an absorption heat pump. Energy 2011:36:3878-87.
- El-Emam RS, Dincer I. Thermodynamic and thermoeconomic analyses of seawater reverse osmosis desalination plant with energy recovery. Energy 2014:64:154-63
- Rensonnet T, Uche J, Serra L. Simulation and thermoeconomic analysis of different configurations of gas turbine (GT)-based dual-purpose power and desalination plants (DPPDP) and hybrid plants (HP). Energy 2007;32:1012-23.
- [8] Penate B, García-Rodríguez L. Energy optimisation of existing SWRO (seawater reverse osmosis) plants with ERT (energy recovery turbines): Technical and thermoeconomic assessment. Energy 2011;36:613-26.
- [9] Fiorini P, Sciubba E. Modular simulation and thermoeconomic analysis of a multi-effect distillation desalination plant. Energy 2007:459-66.
- [10] Selbaş R, Kızılkan O, Şencan A. Thermoeconomic optimization of subcooled and superheated vapor compression refrigeration cycle. Energy 2006;12:2108–28.
- [11] Alkan MA, Kecebas A, Yamankaradeniz N. Exergoeconomic analysis of a district heating system for geothermal energy using specific exergy cost method. Energy 2013;60:426-34.
- Janghorban Esfahani I, Yoo CK. Exergy analysis and parametric optimization of three power and fresh water cogeneration systems using refrigeration chillers. Energy 2013;59:340-55.
- [13] Janghorban Esfahani I, Kim JT, Yoo CK. A cost approach for optimization of a combined power and thermal desalination system through exergy and environmental. Ind Eng Chem Res 2013;52:11099-110.
- Kaita Y. Thermodynamic properties of lithium bromide-water solutions at high temperature. Int J Refrig 2001;24:374-90.
- Misra RD, Sahoo PK, Gupta A. Thermoeconomic evaluation and optimization of a double-effect H2O/LiBr vapour-absorption refrigeration system. Int J Refrig 2005;28:331-43.
- [16] Lazzaretto A, Tsatsaronis G. SPECO: a systematic and general methodology for calculating efficiencies and costs in thermal systems. Energy 2006;31:1257-89.
- [17] Mistra RD, Sahoo PK, Gupta A. Thermoeconomic optimization of a single effect water/LiBr vapour absorption refrigeration system. Int J Ref 2003;26:158-69.
- [18] Bejan A, Tsatsaronis G, Moran M. Thermal design and optimization. New York: John Wiley and Sons; 1996.

## Glossary

A: absorber

ABHP: absorption heat pump

BPE: boiling point evaluation, °C

C: cost rate, \$/s

c: average cost rate, \$/GI

Con.: condenser Com.: compressor

cp: specific heat capacity, kI/kg°C

CFR: cooling fresh water ratio

D: distillate, kg/s

ex: specific exergy, kJ/kg E: exergy rate, kW

Ex: exergy, kJ

EV: expansion valve

f: exergoeconomic factor

F: fuel, kW

G: generator

h: specific enthalpy, kJ/kg

HP: high pressure

L: latent heat

LP: low pressure

LT-MEE: low temperature-multi effect evaporation

MEE: multi-effect evaporation

m: mass flow rate, kg/s

mf mass fraction

MEE-ABHP: multi effect evaporation-absorption heat pump

r: relative cost difference

RR: refrigerant flow-rate ratio

s: specific entropy, kJ/kg K SHX: solution heat exchanger

n: number of effects in the MED-TVC system

P: pressure, bar

O: heat flow rate

Q<sub>fresh water</sub>: fresh water flow rate

T: temperature, °C

VCR: vapor compression refrigeration

W: power, MW

Z: capital cost rate, \$/s

## Subscripts

amb: ambient

A: absorber

CI: capital investment

D: destruction

f: feed water F: fuel

in: inlet stream

k: component

L: loss

OM: operating and maintenance

out: outlet stream

ph: physical P: product

s: salt

sw: seawater

w: water